11th International DAAAM Baltic Conference
"INDUSTRIAL ENGINEERING"
20-22 April 2016, Tallinn, Estonia

DETECTION EFFICIENCY CALIBRATION OF SI-SPAD DETECTORS VIA COMPARISON WITH A Si-STANDARD DIODE

Dhoska, K.; Hofer, H.; López, M.; Rodiek, B.; Kübarsepp, T. & Kück, S.

Abstract: *This paper will focus on improvement of the measurement setup for detection efficiency calibration of Si-SPAD detectors by including a complete automation of the calibration facility, an improved in-situ measurement of the filter transmission and a reduction of the stray light effect in the setup. The improvement yields a reduction in the measurement uncertainty down to 0.2 % at a wavelength of 770 nm.*

Key words: Si-SPAD detector, detection efficiency, calibration, alignment, measurement uncertainty.

1. INTRODUCTION

The Silicon single-photon avalanche diode is one of the most used single-photon detectors due to its stability, robustness, price and easy handling. It is used in many applications and fields of scientific research such as experimental quantum optics, quantum cryptography, quantum computing, 3D-imaging, vision technologies, medicine, biology, astrophysics and telecommunication. The detection efficiency of the Si-SPAD detector is a key parameter in all the fields mentioned above. In order to achieve reliable, reproducible and traceable measurements, the Physikalisch-Technische Bundesanstalt (PTB), the German National Metrology Institute, established a measurement setup for the detection efficiency calibration of Si-SPAD detectors [1-3]. The new configuration setup for determination of the detection efficiency is shown in the Fig.1.

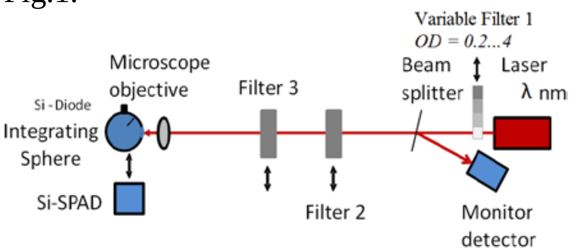

Fig. 1. Schematic view of the calibration setup for Si-SPADs by using an integrating sphere with an attached Si-detector as a reference standard detector [1, 2].

In the calibration process, the alignment of the Si-SPAD detector with respect to the absolute position and to the reproducibility to re-align is of prime importance. The alignment position of the Si-SPAD active area to the incident beam has to be carried out with high accuracy to achieve low uncertainty measurements [4]. An alignment position of the Si-SPAD detector in a completely automated way will play important role for making calibration facility in completely automated way. An integrating sphere with attached Si-standard diode and Si-SPAD detector type Perkin-Elmer SPCM-AQR with diameter 180 µm [5] has been used for detection efficiency calibration. This paper will focus on the improvement of this measurement setup by including a complete automation of the calibration facility, an improved in-situ measurement of the filter transmission and a reduction of the stray light effect in the setup. The improvement yields a reduction in the measurement uncertainty down to 0.2 % at a wavelength of 770 nm.

2. MEASUREMENT PROCEDURE

The measurement procedures consists firstly in alignment position in completed automated way for setting the Si-SPAD detector prior starting the calibration process of the Si-SPAD detector and secondly the measurement procedure for determination the detection efficiency of the Si-SPAD detector.

The alignment of the Si-SPAD detector with respect to the focused beam is carried out using motorized XYZ-translation stages in an automatic manner. This is carried out in three steps: First, two beam profile measurements are carried out by performing a *xy*-scan using the Si-SPAD itself. These scans are performed in front of and behind the objective focal plane. These two scans profile corresponds to Gaussian profile. Although the absolute location of the focal plane it not exactly known, it can be roughly estimated, so that the scan positions for these two scans are easily found. Using this information, the focal plane *f* of the microscope objective is calculated by approximating the beam profile to a simple geometric beam propagation, see dashed line in Fig. 2:

$$f = \frac{d_1 \cdot Z_2 + d_2 \cdot Z_1}{d_1 + d_2}, \qquad (1)$$

where *f* is the objective focal plane, Z_1, Z_2 are the scan positions in the *z*-axis and d_1, d_2 are the beam profile diameters, respectively. Third, a *xy*-scan is performed at the calculated focus position. In this case the obtained scan profile corresponds to a rectangular distribution, because here the active area of the Si-SPAD detector is much larger than the laser beam profile.

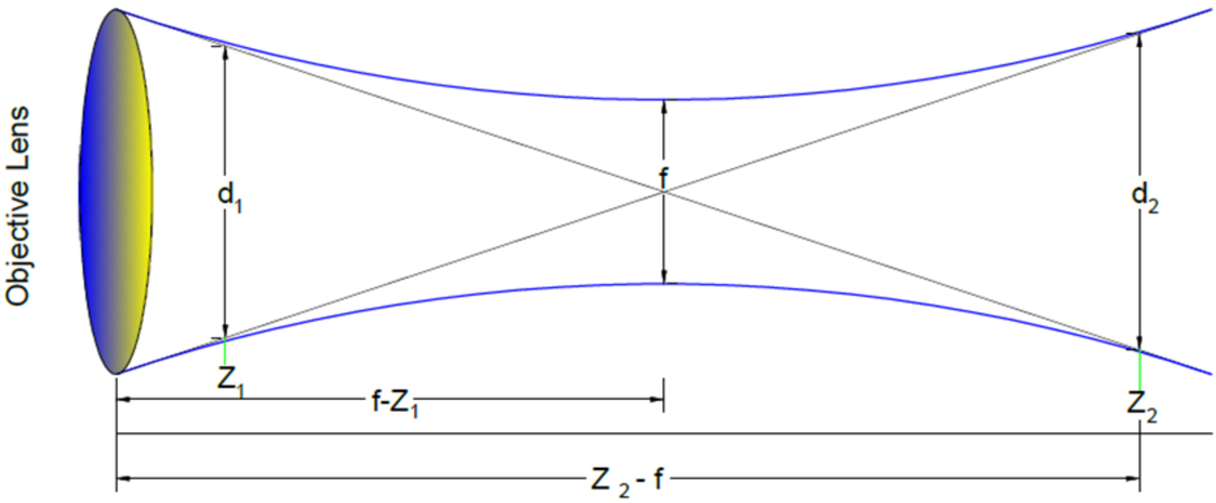

Fig. 2. Schematic view for the determination of the objective focal plane, where *f* is objective focal plane, d_1 and d_2 are beam diameter and z_1 and z_2 are beam distances.

The centre of the rectangular profile is calculated using the centroid algorithm [6], expressed below for *x*- and *y*-coordinates, respectively:

$$x_{center} = \frac{\sum_{i=1}^{N} x_i \cdot s_i}{\sum_{i=1}^{N} s_i}, \qquad (2)$$

$$y_{center} = \frac{\sum_{i=1}^{N} y_i \cdot s_i}{\sum_{i=1}^{N} s_i}, \qquad (3)$$

where s_i are the detector signals and x_i, y_i are the scanning positions in *x*- and *y*-coordinates. The diameters of each rectangular beam profile ($x_{diameter}$ and $y_{diameter}$) are determined by:

$$x_{diameter} = x_{i,\max} - x_{i,\min}\,, \qquad (4)$$

$$y_{diameter} = y_{i,\max} - y_{i,\min}\,, \qquad (5)$$

where $x_{i,max}$ ($x_{i,min}$) is the maximum (minimum) position of the beam diameter in *x*-coordinate direction and $y_{i,max}$ ($y_{i,min}$) is the maximum (minimum) position of the beam diameter in *y*-coordinate direction.

The procedure used for determining the Si-SPAD detection efficiency at PTB is described in detail in [1]. Unlike in [1], in this case an integrating sphere with attached Si-photodiode is used as a standard detector for measuring the optical flux as well as the filter transmission, see Fig. 1. The total filter transmission cannot be measured directly with the standard detector used in our measurement setup, because of the high attenuation. Therefore, a two-step in-situ procedure is used, as described in detail in [1,4]. In the measurement, the filter transmission for each individual filter (T_{F2} and T_{F3}) is measured. Then, in the second step, the overall transmission of the filter combination ($T_{combined}$) is measured, where both filters are simultaneously positioned in the beam path. For a wavelength dependent investigation, a tunable laser source operating in a wavelength range 770 nm is used for the investigation. The deviation between the total filter transmission calculated from the individual filter transmission measurements and the directly determined total filter combination was evaluated by:

$$Dev = 1 - \frac{T_{F_2} \cdot T_{F_3}}{T_{Combined}}\,, \qquad (6)$$

This deviation is taken as the overall uncertainty contribution of the filter transmission for the determination of the detection efficiency of Si-SPAD detectors, as already described in [1,2].

3. MASUREMENT RESULTS

The results for alignment position of the Si-SPAD detector with respect to the different *z*-positions are shown in Fig. 3.

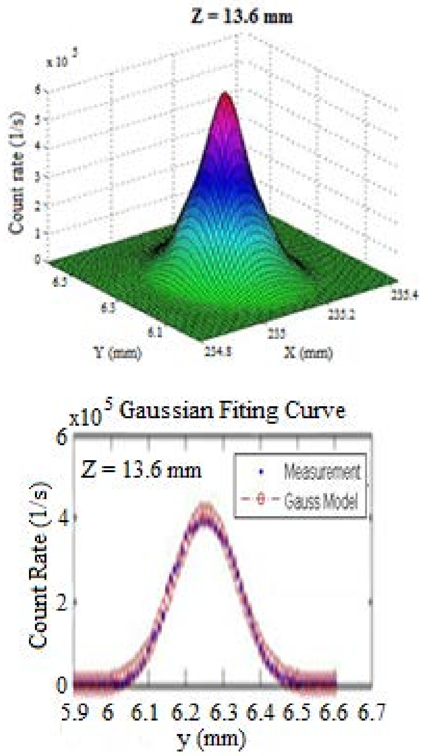

(a)

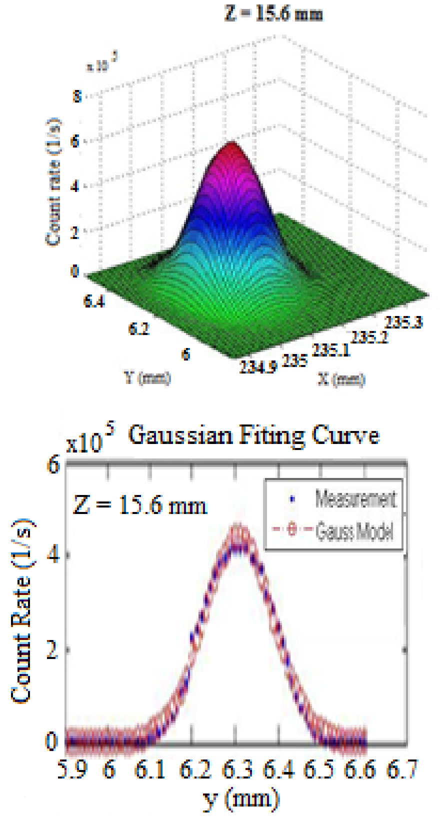

(b)

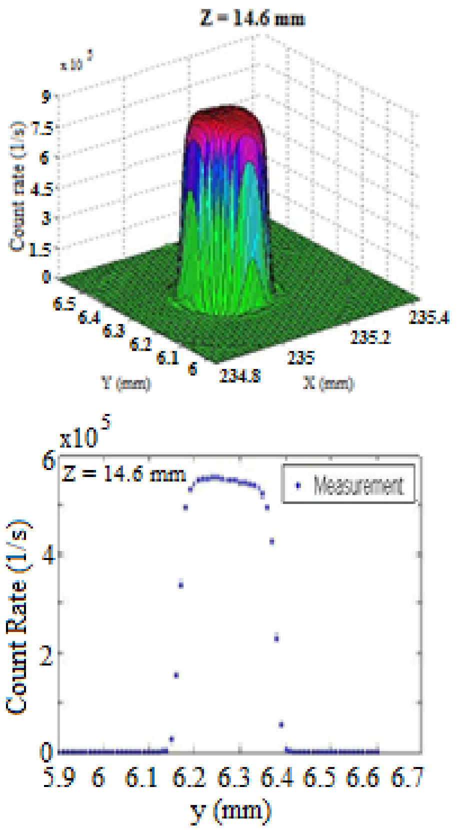

(c)

Fig. 3. Scanning results for different *z* -position of the SPCM-AQR (PerkinElmer) detector. (a) and (b) Scan in front of and behind the focal plane, i.e. predominantly Gaussian profiles with their fitting curves and (c) Scan at focal plane and therefore rectangular profile.

For the *z*-position of 13.6 mm, i.e. closer to the microscope objective than the focal plane, the scan profile corresponds dominantly to a Gaussian beam profile, see Fig. 3a. A second *xy*-scan was performed at a *z*-position of 15.6 mm, i.e. farer away from the microscope objective than the focal plane, see Fig. 3b. Based on these scans and the determined data, the optimum (*x*,*y*,*z*)-position for the detector is calculated to x_{center} = 235.11 mm, y_{center} = 6.28 mm and *z* = 14.6 mm using eq. (1) – (3). As expected, the scan profile at this *z*-position corresponds dominantly to a rectangular profile, see Fig. 3c.

4. DETECTION EFFICIENCY AND ITS ACCOMPANIED UNCERTAINTY

The determination of the detection efficiency of the Si-SPAD accompanied with all possible contribution factors for evaluation of the measurement uncertainty is given by [4],

$$\eta = \frac{hc}{\lambda}\frac{A_2 A_3}{A_1}\frac{Q_1 Q_4}{Q_2 Q_3} s_{Si} F_{filt}\,, \qquad (2)$$

where η is the detection efficiency of the SPAD; i.e. the measurand value, h is the Planck constant, c is the speed of light, λ is the wavelength, A_1, A_2, A_3 are the signal amplification factors, Q_1, Q_2, Q_3 are the ratios of the signal of the Si-diode attached to the integrating sphere and the monitor detector signal, Q_4 is the ratio of the counter and the monitor detector signal, s_{Si} is the spectral responsivity of the integrating sphere with the attached Si-diode, and F_{filt} is the factor taking into account the use of two filters.

All the components listed above and their associated measurement uncertainties were described in detail at [1]. Therefore, in this paper we focus only on those factors and uncertainty components, which were improved. The improvement has been focused in the filter transmission measurement which will reduce one of the major type B components drastically. Based on the equation (6) the maximum deviation for the wavelength 770 nm correspond to 0.03 %. This deviation is used, for simplicity, for the estimation of the uncertainty of the correction factor F_{Filt} for the above wavelength. Thus, the standard uncertainty of the correction factor that uses two filters is estimated:

$$u_{F_{Filt}} = \frac{T_{Individual} - T_{combined}}{T_{combined}\cdot\sqrt{3}} = 3.1\cdot 10^{-4}\,. \quad (7)$$

The uncertainty contribution of the factor which uses two filters is obtained:

$$u_c(F_{Filt}) = \sqrt{c_{Filt}^2 \cdot u_{F_{Filt}}^2} = 9.4\cdot 10^{-4}\,, \qquad (8)$$

where sensitivity coefficient is c_{Filt} = 0.64. The new contribution value of the factor using two filters is included into the uncertainty budget and is used to estimate the combined uncertainty $u_c(\eta)$ [1,2].

Finally, the obtained detection efficiency of the Si-SPAD detector is:

$$\eta_{SPAD} = 0.5968 \pm 0.001,$$
$$\eta_{SPAD} = 0.5968 \pm 0.16\ \%.$$

5. CONCLUSIONS

In this paper, the improvement of the measurement setup by including a complete automation of the calibration facility was described. These improvements are based on the optimization of the Si-SPAD detector positioning, which is now performed in a completely automated way. The improved relative standard uncertainty of the detection efficiency of the Si-SPAD was 0.16 %.

6. REFERENCES

1. M. López, H. Hofer, S. Kück, Detection efficiency calibration of single-photon silicon avalanche photodiodes traceable using double attenuator technique, *Journal of Modern Optics*, 2015, **62**, S21-S27.
2. K. Dhoska, H. Hofer, M. López, B. Rodiek, T. Kübarsepp, S. Kück, S. High accuracy filter transmission measurement for determination of the detection efficiency calibration of Si-SPAD detectors, In: *Proceedings of DAAAM Baltic: 10th International DAAAM Baltic Conference "Industrial Engineering"*, (Otto, T., ed.) Tallinn, Estonia, 2015, 123-127.
3. K. Dhoska, H. Hofer, M. López, T. Kübarsepp, S. Kück, Improvement of the detection efficiency calibration of Si-SPAD detectors and investigation of the detection efficiency homogeneity, *MAPAN-Journal of Metrology Society of India*, *Springer*, Submitted.
4. K. Dhoska, H. Hofer, M. López, T. Kübarsepp, S. Kück, Alignment position method for SPAD detector calibration and homogeneity, *International Journal of Scientific Reports*, 2015, **1 (7)**, 271-274.
5. Perklin Elmer SPCM-AQR Detector. Single Photon Counting Module http://www.pas.rochester.edu/~advlab/APD_SPCM_AQR.pdf, Accessed 31 March 2016.
6. D. R. Neal, R. J. Copland, D. A. Neal, D. M. Topa, and P. Riera, Measurement of lens focal length using multi-curvature analysis of Shack-Hartmann wavefront data, *Proc. SPIE*, 2004, *5523*, 243-256.

7. ADDITIONAL DATA ABOUT AUTHORS

Klodian Dhoska, doctoral student,
Department of Mechatronics, Tallinn University of Technology, Ehitajate tee 5, 19086, Estonia.
Email: klodian.dhoska@ttu.ee

Helmuth Hofer, engineer,
Division of Optics, Physikalisch-Technische Bundesanstalt (PTB), Bundesallee 100, 38116 Braunschweig, Germany.
Email: helmuth.hofer@ptb.de

Beatrice Rodiek, doctoral student,
Division of Optics, Physikalisch-Technische Bundesanstalt (PTB), Bundesallee 100, 38116 Braunschweig, Germany.
Email: beatrice.rodiek@ptb.de

Marco López, doctor,
Division of Optics, Physikalisch-Technische Bundesanstalt (PTB), Bundesallee 100, 38116 Braunschweig, Germany.
Email: marco.lopez@ptb.de

Toomas Kübarsepp, professor,
Department of Mechatronics, Tallinn University of Technology, Ehitajate tee 5, 19086, Estonia.
Email: toomas.kubarsepp@ttu.ee

Stefan Kück, professor,
Division of Optics, Physikalisch-Technische Bundesanstalt (PTB), Bundesallee 100, 38116 Braunschweig, Germany.

Email: stefan.kueck@ptb.de

8. ACKNOWLEDGEMENT

This research work has been supported by the project “Single-Photon Sources for Quantum Technology” (SIQUTE) with Researcher Mobility Grant (RMG) EXL01-RMG1 of the European Metrology Research Programme (EMRP). The EMRP is jointly funded by the EMRP participating countries within EURAMET and the European Union.